Received: 11 February 2021 | Revised: 20 August 2021 | Accepted: 17 November 2021

DOI: 10.1111/jfr3.12778

ORIGINAL ARTICLE

CIWEM Chartered Institution of Water and Environmental Management | Journal of Flood Risk Management | WILEY

Transposing flood risk from extreme rainfall events: A case study of Hurricane Harvey

Elizabeth Regier | **Joseph Naughton** | **Walter McDonald**

Department of Civil, Construction, and Environmental Engineering, Marquette University, Milwaukee, Wisconsin, USA

Correspondence
Walter McDonald, Department of Civil, Construction, and Environmental Engineering, Marquette University, 1515 W. Wisconsin Ave. Milwaukee, WI 53233, USA.
Email: walter.mcdonald@marquette.edu

Abstract

Hurricane Harvey produced unprecedented flooding that altered flood frequency statistics near Houston, Texas. While Harvey could have made landfall elsewhere along the Gulf coast, traditional flood frequency methodologies only consider the risk of Harvey in the region that it hit. This may be a shortcoming of flood frequency methodologies as the intensity of Harvey was greater due to climate change; therefore, Harvey may be more indicative of future hurricanes than other historical observations. To that end, this study investigates what effect Harvey would have had on flood frequency statistics if it had made landfall elsewhere. To do so, a Monte Carlo simulation was used to shift Harvey's rainfall within alternative landfall locations. This rainfall was then applied to synthetic unit hydrographs to estimate peak flows that were applied in Log Pearson III and Regional Flood Frequency Analyses. Log Pearson III analyses with simulated Harvey streamflows produced median 100-year peak flows that were 17%–66% higher than analyses that only used historical records. A regional flood frequency analysis in the central coastal geomorphologic region of Texas showed that predictive equations, based upon basin area and shape factor, had an average increase of 30.2% in the 100-year peak discharge.

KEYWORDS

flood frequency, flood risk, hurricanes, peak flows, regional regression, return periods

1 | INTRODUCTION

Hurricane Harvey hit the coast of Texas on August 25, 2017, bringing high winds and torrential rainfall with a reported maximum measured rainfall of 1539 mm (60.58 in.) in the Netherlands, Texas (Blake & Zelinsky, 2017). This rainfall, paired with winds up to 59.2 m/s, resulted in at least 68 direct deaths, 35 indirect deaths, and $125 billion of damage (2017). It is estimated that approximately 8%–19% of Hurricane Harvey's intensity was attributed to climate change (Risser & Wehner, 2017; van Oldenborgh et al., 2017). This intensity had a significant impact on the computation of design floods, as the flooding from Harvey increased the 100-year peak flow in the region by an average of 28% using flood frequency statistics (McDonald & Naughton, 2018).

Flood frequency statistics use historical records of annual maximum instantaneous peak discharge to estimate the magnitude and frequency of peak floods. These estimates can then be applied within regional flood frequency analysis to develop equations that predict the

magnitude and frequency of peak discharges based upon basin characteristics. These predictions of peak discharge are critical for the safe design of civil infrastructure such as dams, levees, bridges, roads, and culverts. Recommended procedures for regional flood frequency analysis have been provided by Bulletin 17B (Rallison et al., 1981), which in March 2018 the United States Geological Survey (USGS) updated as Bulletin 17C (England et al., 2019). While the updated procedures acknowledge concerns surrounding the effect of climate change on flood frequency, the recommended methods still assume stationarity within the data. Given studies showing the impact of climate change on Harvey (e.g., Hassanzadeh et al., 2020; van Oldenborgh et al., 2017), we know this is not the case for recent storms (Marsooli et al., 2019; Reed et al., 2020). This is important to consider, as extraordinary storms such as Harvey have a significant influence on the flood frequency statistics and therefore are critical in developing regional flood frequency equations.

Incorporating climate change into flood frequency analyses would be a prudent approach; however, doing so is a significant challenge due to the reliance of flood frequency analysis on empirical data. While there are no guidelines for incorporating climate change into flood frequency analysis, Bulletin 17C does offer suggestions (England et al., 2019). One is a method that couples a Bayesian statistical approach with a reversible jump Monte Carlo Markov Chain procedure to develop a nonstationary precipitation frequency analysis from past data in a single location; however, this methodology does not propose a way to translate this modeled precipitation into streamflow (Ouarda & El-Adlouni, 2011). Another method calculates flood magnification factors (e.g., a factor of 2 for the 100-year flood indicates that the 100-year flood will increase two-fold) and recurrence reduction factors (e.g., a factor of 2 for the 50-year flood indicating that the 50-year flood will become the 25-year flood) for specific basins nationwide using their respective streamflow data (Vogel et al., 2011). However, this method does not separate out the multiple sources of nonstationarity, such as climate change and land-use change. Beyond those listed in Bulletin 17C, other methods exist, many of which utilize climate models (e.g., Griffis & Stedinger, 2007; Srivastav et al., 2014). While these methods provide opportunities for the inclusion of climate change into flood frequency analysis, there is an overall lack of consensus on how to do so.

This lack of consensus has led to applications of flood frequency methods that still assume stationarity in the data. This is a significant shortcoming as it is generally accepted that extreme precipitation events exhibit nonstationary patterns (Vu & Mishra, 2019). By not accounting for these patterns, current methods for hydrologic design of infrastructure, such as flood frequency analysis and regional regression, are poorly suited for considering risk from nonstationarity of extreme events (Wright et al., 2019). In addition, extreme flooding events are increasingly being attributed to hurricanes (Dhakal & Jain, 2019), which presents challenges for flood frequency statistics in coastal regions. Therefore, alternative approaches to flood frequency are needed to consider the influence of peak flows from climate enlarged hurricanes.

In this study, we present an approach to address this challenge by transferring flood risk from observed hurricanes to alternative basins within their modeled landfall paths through rainfall transposition. Rainfall transposition has been applied to augment radar rainfall data for frequency estimations of extreme rainfall (Wright et al., 2013), in synthesizing long records of rainfall (Wright et al., 2014), and in explore thing relationship between peak discharges and spatial moments of rainfall (Gao & Fang, 2018). Here we apply it to transfer the flood risk from Hurricane Harvey to other locations within its modeled landfall path. Because traditional flood frequency analysis is empirical, the risk from these hurricanes in a flood frequency analysis is only considered within the regions that they hit. However, in the case of Harvey, hurricane prediction models showed that it could have made landfall in numerous locations along the Gulf coast (Huttner, 2017). In these locations, Harvey may be more indicative of current and future hurricanes than other historical observations due to the influence of climate change on its intensity.

To that end, the objective of this study is to present a method to transfer flood risk from hurricanes to other geographical areas within their modeled landfall path. To do so, we applied the proposed method to Hurricane Harvey to evaluate what impact it would have had on flood frequency statistics and regional regression equations had its precipitation occurred elsewhere. Specifically, we (i) evaluated the probabilistic landfall locations for Harvey using the Global Forecast System (GFS) and the Meteorological Office Global and Regional Ensemble Predictions System (MOGREPS-G) ensemble models from Hurricane Harvey, (ii) shifted the spatial rainfall data from Harvey to two probabilistic locations using a Monte Carlo simulation, (iii) applied a synthetic unit hydrograph method to simulate peak flows from Harvey, (iv) developed flood frequency statistics using the simulated peak flows and Bulletin 17C methodologies, and (v) integrated these flood frequency statistics into a regional flood frequency analysis. Through this study we hope to contribute to the discussion surrounding the importance of considering alternative approaches to flood frequency statistics.

2 | MATERIALS AND METHODS

2.1 | Development of path probability distribution

To determine the alternative locations where Hurricane Harvey could have made landfall, we evaluated ensemble hurricane track forecasts. Specifically, we used ensemble hurricane track forecasts to develop probabilistic landfall maps at 1, 2, 3, and 4 days before landfall. Ensembles included 6-h interpolations of the United States-based GFS ensemble (20 ensemble members) and United Kingdom-based UKMET MOGREPS-G ensemble (36 ensemble members) that were downloaded from the Automated Tropical Cyclone Forecasting System (ATCF) database (ATCF, 2017). Probabilistic landfall for any given point on the coast was computed using the following equation:

$$P = \frac{M_{\text{Distance}}}{M_{\text{Total}}} \tag{1}$$

where M_{Distance} is the number of ensemble members coming within 111 km or 60 nautical miles distance of a given point (Sheets, 1985); M_{Total} is the total number of ensemble members; and P is the probability that the center of the hurricane's eye will come within the designated distance of a given point. Some ensemble member predictions ended before making landfall on the western side of the Gulf of Mexico, and because our focus was on landfall locations, these were not included in our analysis.

2.2 | Shifted Harvey rainfall data

The precipitation data from Harvey was generated from a total of 963 precipitation gages in southeast Texas from the National Weather Service and National Oceanic and Atmospheric Administration (NOAA). From these point gages, inverse distance weighting was used to develop a map of the 3-day rainfall total. Then two new regions were selected for transposing the 3-day rainfall using region boundaries defined by the USGS (Asquith & Slade, 1997). The two regions were selected based upon their location within the probabilistic landfall path and data availability. Potential regions were restricted to those that fell within the 25% probability range of landfall based upon ensemble forecasts. The selected regions also were required to not be heavily impacted by the original storm. Finally, each geomorphologic region needed to have an adequate number of stream gages with 10 or more years of data and in operation beyond the year 2000.

Once the two geomorphologic regions were selected, the 3-day precipitation map was transposed to these regions using a Monte-Carlo simulation. Using ESRI ArcMap (Esri Inc., 2017), the 3-day precipitation was transposed to locations within each defined geomorphologic region ($n = 1500$). The simulation randomly generated latitude and longitude of the rainfall map under the constraint that its centroid fell within the region boundaries. Then using the transposed location, the volume of rainfall over the watershed of each stream gage was computed. Finally, the median rainfall volume that fell over each watershed from the 1500 simulations was used to estimate peak runoff, as described in the following section.

2.3 | Estimating peak flows using a synthetic unit hydrograph

The median rainfall volume over each watershed from the Monte Carlo simulations were used to estimate peak flows through a synthetic unit hydrograph approach. Synthetic unit hydrographs define the hydrograph of a watershed that would result from 1 in. of rainfall and are commonly applied to estimate peak flows, especially where precipitation and geographic information for a watershed is known but streamflow data is unavailable (Adib et al., 2010; Dawod & Koshak, 2011; Günal & Güven, 2016; Reshma et al., 2010; Sule & Alabi, 2013). Once developed, a synthetic unit hydrograph can be applied to estimate peak discharge for any given storm event based upon the product of the unit hydrograph peak flow ($m^3/s/mm$ or cfs/in.) and the average watershed rainfall in millimeters (or in.).

We estimated peak flows in each watershed using the Soil Conservation Service (SCS) synthetic unit hydrograph method (Ponce, 1989). This is a method to develop a synthetic unit hydrograph based upon drainage area and rainfall duration, as shown in the following equation:

$$T_{\text{L}} = 1.44 \times \left(\frac{A}{2.589}\right)^{0.6} \tag{2}$$

$$T_{\text{P}} = \frac{D}{2} + T_{\text{L}} \tag{3}$$

$$Q_{\text{P}} = \frac{(2.084 \times A)}{T_{\text{P}}} \tag{4}$$

where T_{L} is the lag time in hours; A is the watershed area in square kilometers; T_{P} is the time to peak discharge in

hours; D is the duration of rainfall in hours; Q_P is the unit hydrograph peak discharge in $m^3/(s \times cm)$.

Watershed areas were delineated using elevation data from the USGS National Map Viewer (U. S. Geological Survey, 2019a) within ESRIs ArcMap (Esri Inc., 2017). These watershed areas were then used to estimate a 3-day rainfall volume based upon the median precipitation over the watershed from the Monte Carlo simulations. The 3-day rainfall volume was finally multiplied by Q_P to get the simulated peak flow.

The method was validated using empirical data by applying it to 25 stream gages that were impacted by Harvey in southeast Texas. The total error between the recorded and estimated peak flows were estimated based upon the root mean square error. The total error is assumed to be comprised of two independent error sources—measurement error and synthetic unit hydrograph error—as shown in the following equations:

$$E_T{}^2 = E_M{}^2 + E_{SUH}{}^2 \quad (5)$$

where E_T is the total error in peak flow; E_M is the streamflow measurement error; and E_{SUH} is the synthetic unit hydrograph error.

This equation can be rearranged to estimate the error from the synthetic unit hydrograph using the estimated total error and the measurement error (Di Baldassarre & Montanari, 2009; Harmel et al., 2006):

$$E_{SUH} = \left|\sqrt{E_T{}^2 - E_M{}^2}\right| \quad (6)$$

Once validated, the synthetic unit hydrographs were developed for each of the watersheds in the study. These unit hydrographs were applied to the median rainfall volume from the Monte Carlo simulations to estimate peak discharges at the simulated Hurricane Harvey locations. Finally, the simulated peak discharges at each site were used to evaluate how Harvey changed flood frequency statistics as outlined in the following sections.

2.4 | Log Pearson III analysis

We developed Log Pearson III flood frequency statistics in each of the two simulated landfall regions to determine the impact that Hurricane Harvey may have had on flood frequency statistics had it fallen elsewhere. To do so, we computed flood frequency statistics both before and after simulating peak flows from Harvey. In the latter case, we chose the simulated peak flow from Harvey as our annual maximum for 2017.

We performed Log Pearson III flood frequency analyses using PeakFQ software (Veilleux et al., 2013) and annual peak flow records from USGS gages (U. S. Geological Survey, 2019b). Within the PeakFQ settings, we performed our analysis using the Bulletin 17C Expected Moments Algorithm (EMA) (England et al., 2019). The weighted skew option within Peak FQ was used, which combines the station skew and generalized skew to create a more accurate measurement of the skew coefficient for a given watershed. We obtained our generalized skew values from Plate I of Bulletin 17B, as updated generalized skew values for the Texas had not yet been published at the time of the study. We also applied the Multiple Grubbs-Beck test and included historical peaks in the analysis. To be considered in the analysis, gages were required to be free of damming or diversions during their period of record, have a period of record of at least 10 years, and in operation beyond the year 2000.

Upon the calculation of flood frequency statistics, we compared return period flows before and after simulating Harvey in each region. We then calculated the net change and percent change in these return period flows using Equation (7) below.

$$P = \frac{S - H}{H} \times 100\% \quad (7)$$

where P is the percent change; S is the flow rate from analysis using simulated Harvey peak flow; and H is the flow rate from analysis using only historical observed data.

2.5 | Nonstationarity analysis of peak flow records

In addition to nonstationarity in our data from simulating Harvey, there may be other sources of nonstationarity in the period of record at the gages due to climate or land use changes. We therefore tested our data for nonstationarity using three statistical tests. We tested for abrupt or sudden changes in the data using the Pettitt test. The Pettit test is an adaptation of the rank-based Mann–Whitney statistic that tests whether two samples from the same population (Pettitt, 1979), and it has been effectively applied to detect abrupt changes in flood peak records (Barth et al., 2017; Villarini et al., 2011). We tested for monotonic trends using both the Mann-Kendall and Spearman Rho tests (Helsel & Hirsch, 2002). These two tests are commonly used to detect monotonic trends in flood peaks and using both can provide clearer evidence of a trend or lack thereof in the flood peak records (e.g., Villarini et al., 2009). The significance level for all

tests was set to 5%. Together, these tests evaluate if there is any nonstationarity in our data and help to put our flood frequency analysis results within the greater context of changes to peak flow data within the watersheds in this study.

2.6 | Regional flood frequency analysis

Regional flood frequency analysis was performed to evaluate the impact that changes in flood frequency statistics have on engineering design equations. The southern coast region did not have enough gages for a reliable regional flood frequency analysis that fit the criteria of 10 or more years of data and in operation beyond the year 2000; therefore, the analysis was only performed on the central coast region. The regional flood frequency analysis was modeled in WREG (Eng et al. 2010) to perform logarithmic weighted-least squares multiple-linear regression. Drainage area, basin shape factor (defined as the longest flow length divided by watershed area), and average stream slope were selected as independent variables for stepwise regression. These were selected because they were used within previous flood frequency studies for the regions (Asquith & Slade, 1997). Regional flood frequency analysis methods would usually consider a wide range of basin parameters and develop a final set through stepwise regression methods. However, because the referenced study was performed on the same watersheds and this study is not focused on parameterization methods, we only evaluated this final set of parameters. These variables were developed using ESRIs ArcMap and digital elevation data from the National Elevation Dataset (NED) obtained through the USGS national Map Download Platform (http://viewer.nationalmap.gov/viewer). After we performed weighted-least squares multiple linear regression, we applied the regression equations to the range of drainage areas and basin shape factors in the

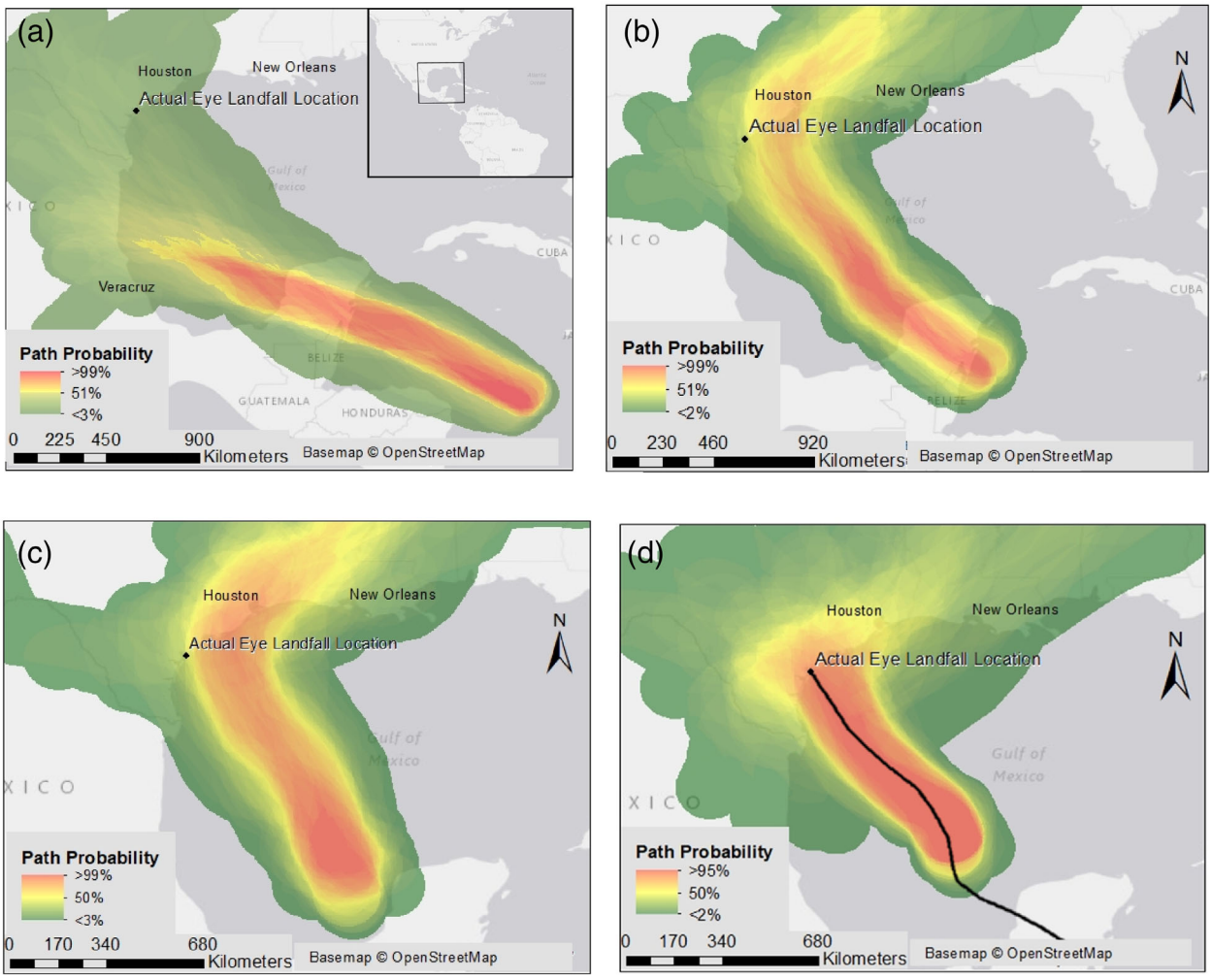

FIGURE 1 Harvey path probability distributions for (a) August 21, 2017, (b) August 22, 2017, (c) August 23, 2017, and (d) August 24, 2017. The black line in (d) represents Harvey's actual path. (source: https://www.nhc.noaa.gov/)

study area to evaluate the impact that simulating Harvey would have on engineering design.

3 | RESULTS

3.1 | Probabilistic and simulated landfall locations

Probability distribution maps of Harvey's projected path were created using the GFS and UKMET MOGREPS-G ensemble forecasts during each of the 4 days preceding Hurricane Harvey's landfall (Figure 1). These maps show the probability that the center of Harvey's eye would have come within 111 km (60 nautical miles) of any given location. In each frame, yellow to red shades show where Hurricane Harvey's eye was more likely to hit, while green shades represent regions where Harvey's eye was less likely to hit. Regions without any coloration had a near-zero chance of encountering Harvey's eye.

The probable landfall locations varied considerably along the Gulf Coast from Veracruz Mexico to New Orleans, LA over the span of four days. For example, on August 21, 2017, Hurricane Harvey's most probable path was near Veracruz, significantly south of where Harvey actually hit on August 25 (Figure 1a). The following days on August 22 and 23, the most probable path showed Harveys landfall shifting north to near Houston, TX (Figure 1b,c) before shifting south of Houston 1 day out on August 24th. Not only do the modeled landfall locations move considerably over time but the ensemble forecasts cover a significant geographic area, with the predicted landfall locations even a day out covering the entire Texas coast (Figure 1d). Given this variability, we sought to evaluate the impact that Harvey could have on flood frequency statistics if its significant rainfall had happened elsewhere along the Texas coast.

Two regions were selected for transposing Harvey's precipitation data within its probabilistic flow path. These locations were chosen based upon regionalization of the state of Texas in a previous flood frequency analysis study (Asquith & Slade, 1997). This study divided Texas into 11 different geomorphologic regions, three of which are aligned along the Gulf Coast of Texas. As shown in Figure 2, Harvey's greatest precipitation occurred in the northern coastal region. The other two coastal regions—central and southern—also met the criteria of stream flow gages with adequate periods of record.

Once the two regions were selected, a Monte-Carlo analysis was performed by randomly transposing rainfall data within each region ($n = 1500$) and then computing the median 3-day precipitation that fell over each watershed. Results found an average median 3-day precipitation amount of 58 cm (southern) and 67 cm (central) with an average coefficient of variation of 0.19 (southern) and 0.25 (central) (Figure 3). The median 3-day precipitation amounts over each watershed were then used to develop synthetic unit hydrographs to simulate peak flows from transposing Harvey as outlined in the following section.

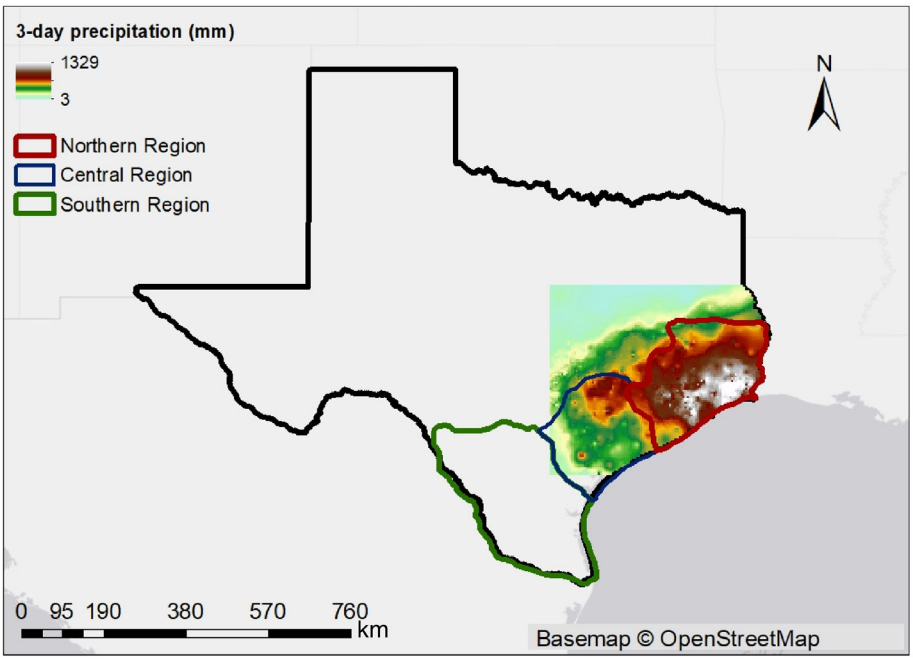

FIGURE 2 Map of the northern, central and southern geomorphologic regions, along with the actual 3-day precipitation from Hurricane Harvey

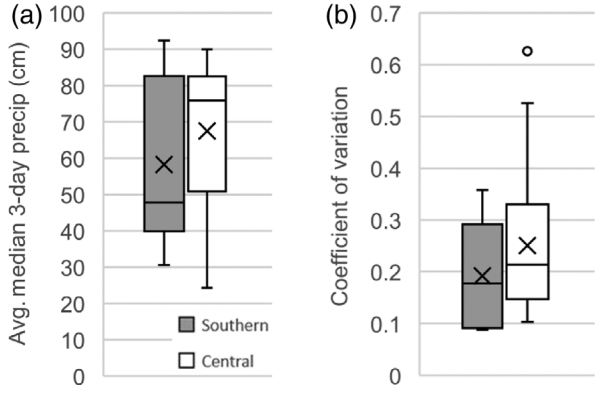

FIGURE 3 Distribution of the (a) median 3-day precipitation and (b) coefficient of variation across all gages in the Southern and Central regions

3.2 | Synthetic unit hydrographs

On average, the absolute error between the measured peak flow and that predicted by the SCS method was 44% (Figure 4). While some of this error resulted from the synthetic unit hydrograph method itself, it is likely that much of it came from streamflow measurement error. Because Harvey was an extraordinary storm, many of the flow rate estimates would be derived from water levels that exceed the calibrated range of their stage-discharge rating (Turnipseed & Sauer, 2010), which could result in significant errors in the discharge estimates (Cook, 1987; Kuczera, 1996). Estimates of streamflow measurement error in general range between 10% and 20% (Harmel et al., 2006); however, for extreme events the discharge measurement error may be closer to 42.8% for a 100-year flood (Di Baldassarre & Montanari, 2009) or even over 100% in streams with high slopes (Jarrett, 1987). While Harvey was significantly greater than a 100-year flood, there is no literature providing estimates of measurement uncertainty at such extremes. Therefore, we explored the potential range in our synthetic unit hydrograph error using 15%–42.8% for the measurement error (E_M) and 44% for the total error (E_T), or the average error between measured and predicted peak flows. We then applied these values to Equations (5) and (6), which resulted in an estimated synthetic unit hydrograph error (E_{SUH}) of 10%–41%. While this is based on an assumption of measurement error during extreme flood events that could in fact be much higher, it provides a general estimate of the potential range in error within our method to produce peak flood based upon transposed precipitation data.

3.3 | Flood frequency statistics

Log-Pearson III analysis was performed on peak stream gage data both with and without simulated Harvey peak flows, and results indicated that Harvey increased the average return period flows across all watersheds. Figure 5 contains box and whisker plots of the percent change in the estimate design floods across all watersheds in both the central and southern region. As shown in the figure, the median return period increases from 3% for the 2-year storm to 17% for the 100-year storm in the central region, and 2% for the 2-year storm to 66% for the 100-year storm in the southern region. We plotted the change in the 100-year peak flow at each gage location to evaluate if these changes clustered geographically (Figure 6). From this figure there were no clear clusters, and large and small changes in the 100-year peak flows were generally distributed throughout the entire study area. These changes in return period floods are similar to

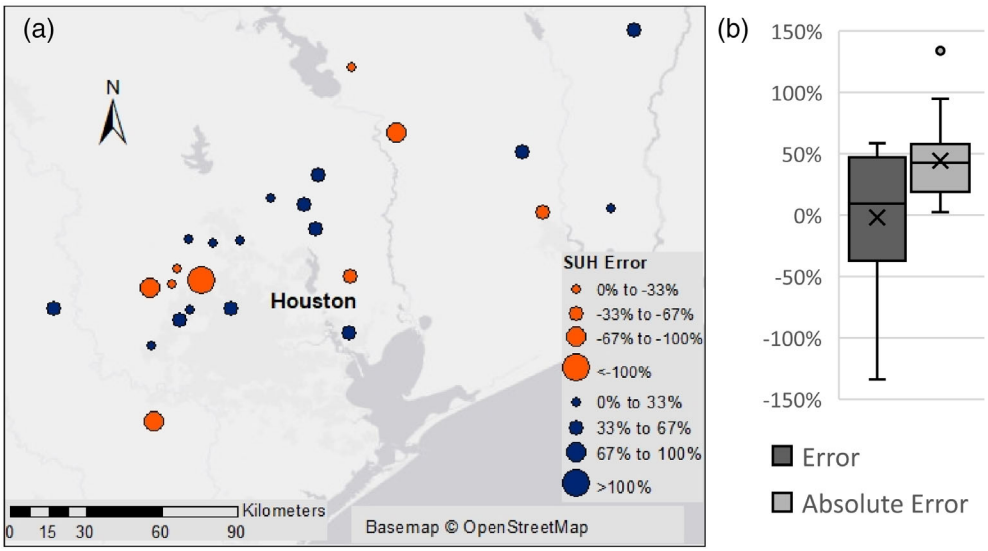

FIGURE 4 (a) Spatial distribution of the northern region SUH error and (b) box and whisker plots of the error and absolute error across all gages

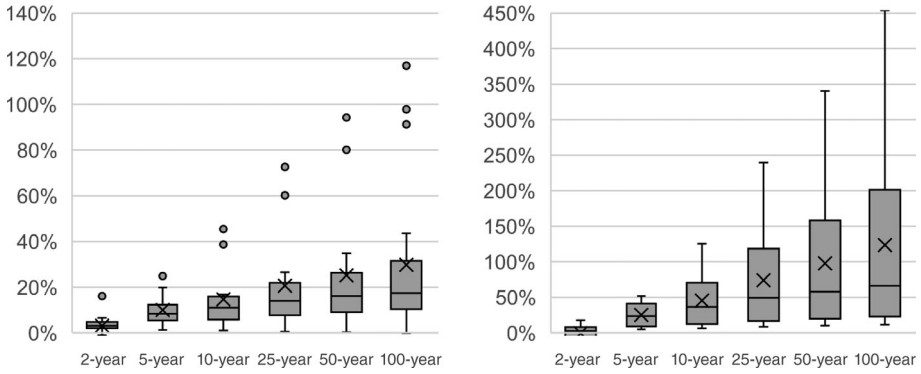

FIGURE 5 Percent change in LPIII flow rates associated with key return periods for the central region (left) and southern region (right)

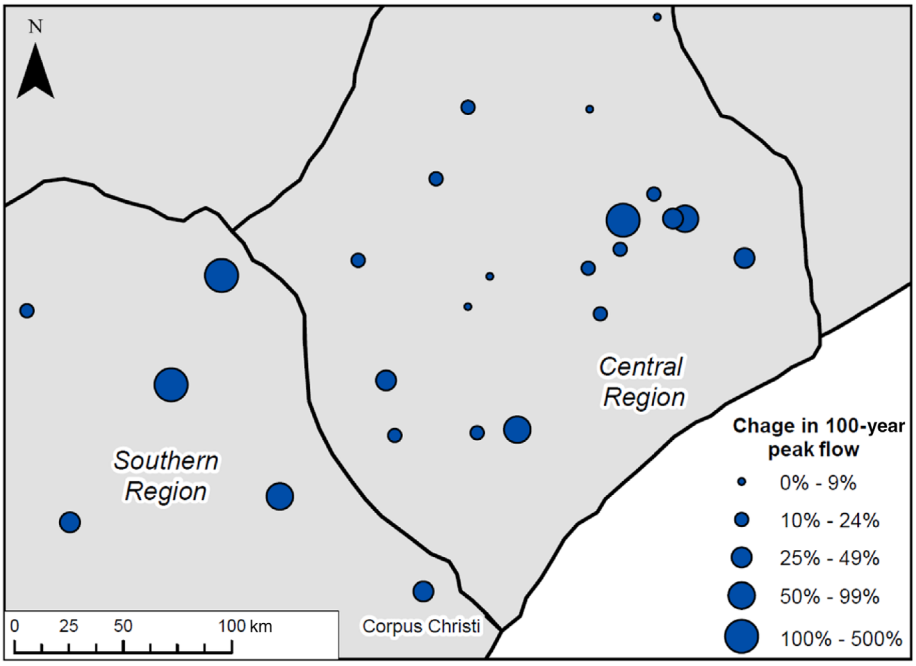

FIGURE 6 Percent change in peak flow rate associated with the 100-year return period for the central and southern regions

those that occurred where Harvey actually made landfall, which resulted in an average increase in the 100-year flood of 30% (McDonald & Naughton, 2018). This outcome demonstrates that the impact of simulating Harvey on flood frequency statistics is similar, and in some cases greater, in other areas along the Texas coast. This is significant for flood risk management as a 17%–66% increase in the 100-year flood could translate to existing infrastructure that is under-designed.

To further explore sources of error within our data, we evaluated the impact that the length of record at our gages had on our analysis. It is known that the period of record may influence flood frequency results by overestimating design flows and resulting in greater error of the estimates (McCuen & Galloway, 2010). To investigate this, we plotted the percent change in return period against years of record for the 5- and 100-year return periods. As shown in Figure 7, the percent difference increases with decreasing years of record. This could be due to greater error of the estimates in gages that have shorter periods of record. However, even in gages that have over 50 years of record, the change in the 100-year return flood in the central region was above 20% in a few cases.

3.4 | Nonstationarity

Stationarity tests were performed and it was found that six of the 26 stations had either an abrupt change or monotonic trend in their data (Table 1). Abrupt changes were detected using the Pettitt test. Monotonic trends were detected with the Mann-Kendall and Spearman Rho tests, with the Spearman Rho test also indicating whether trends were positive or negative. As shown in the table, there were five stations that had a statistically significant abrupt changes ($p \leq 0.05$) and four of these stations also had a negative monotonic

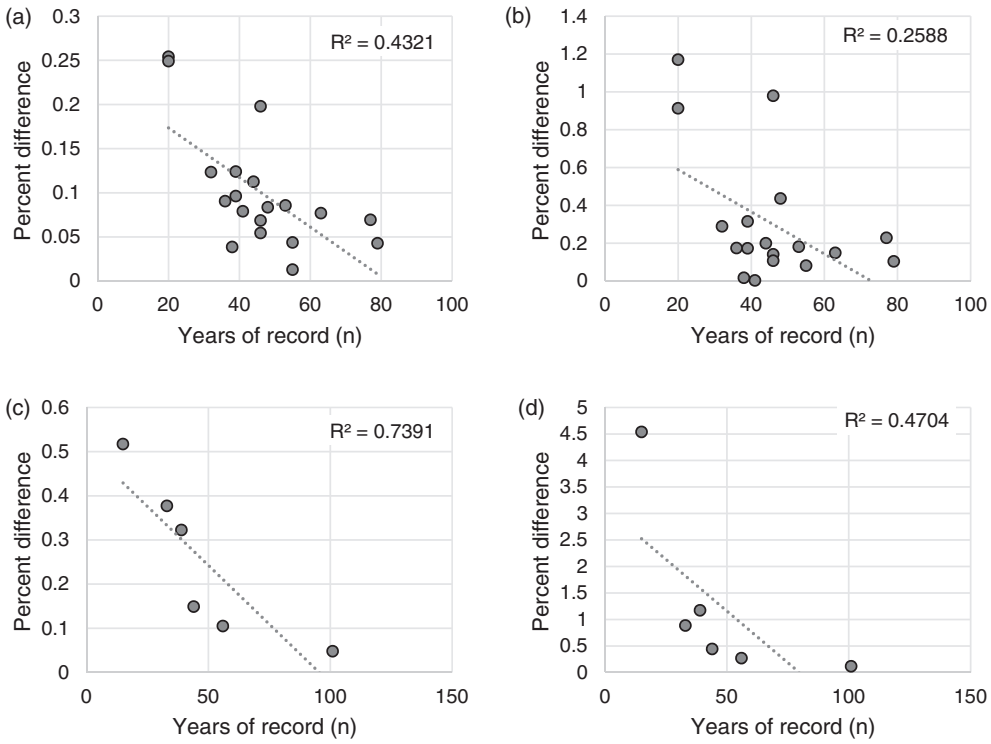

FIGURE 7 Percent change in Bulletin 17C LPIII flow rate against the years of record for (a) the central region 5-year flood; (b) the central region 100-year flood; (c) the southern region 5-year flood; and (d) the southern region 100-year flood

TABLE 1 Pre-2017 nonstationarity test results in the central and southern regions

Region	Station	Pettit year change detected	Pettit *p*-value	Mann-Kendall trend	Spearman Rho trend
Central	08164504	Change in 2004	0.0313	No trend	Negative trend
	08164800	Change in 2000	0.0436	Trend found	Negative trend
	08176900	Change in 1986	0.0499	Trend found	Negative trend
	08177300	Change in 2004	0.0470	No trend	No trend
	08189300	Change in 2004	0.0068	Trend found	Negative trend
Southern	08212400	No sudden change	0.1243	Trend found	No trend

trend. No stations indicated a positive trend, which suggests that these stations have not seen an increase in peak flow rates due to either climate or land use changes.

3.5 | Regional flood frequency analysis

Regional flood frequency analysis was performed in the central region and resulted in equations that estimated return period peak flows based upon drainage area and basin shape factor. The equations shown in Tables 2 and 3 are those from stepwise regression that produced the best model fit through the pseudo R^2, standard model error (SME), and standard error of prediction (Sp), while maintaining significance ($p > 0.05$) for each of the variables used. For most return periods, the regression equations used the same variables in both the historical record analyses and simulated Hurricane Harvey analyses. However, for the 10-, 50-, and 100-year return periods, the historical record regressions utilized drainage area and basin shape factor, while the simulated Harvey regressions utilized only drainage area.

We used these equations to compute predicted peak flows with the basin characteristics within our study and found that this produced an average percent increase in the predicted peak flows of 5.7%, 11.2%, 18.6%, 19.8%, 29.6%, and 30.2%, for the 2, 5, 10, 25, 50, and 100-year storms respectively. Figure 8 illustrates the size of this increase across the range of basin characteristics within our study. Figure 8a shows the percent change in peak flows for the 5-year return period, for which basin drainage area was the only significant independent variable. As illustrated, for the 5-year return period there is a change in peak flow ranging

TABLE 2 Regional flood frequency regressions for the central region record through 2017

Regression equation	Sp (%)	Pseudo R^2	SME (%)
log(2-year Q) = 1.02 + 0.377*log(DA)	62.74	33.62	58.78
log(5-year Q) = 1.18 + 0.455*log(DA)	48.87	54.94	45.8
log(10-year Q) = 1.39 + 0.624*log (DA) − 0.554*log(BH)	39.83	73.47	35.84
log(25-year Q) = 1.46 + 0.693*log (DA) − 0.630*log(BH)	40.22	77.37	35.91
log(50-year Q) = 1.50 + 0.739*log (DA) − 0.678*log(BH)	44.73	76.05	39.91
log(100-year Q) = 1.58 + 0.768*log (DA) − 0.731*log(BH)	51.22	72.55	45.75

Abbreviations: DA, drainage area in km^2; Q, peak flow in m^3/s; BH, basin shape factor (dimensionless).

TABLE 3 Regional flood frequency regressions for the central region record that include simulated Harvey peak flows

Regression equation	Sp (%)	Pseudo R^2	SME (%)
log(2-year Q) = 1.02 + 0.386*log(DA)	64.18	33.69	60.12
log(5-year Q) = 1.21 + 0.461*log(DA)	43.93	60.58	41.13
log(10-year Q) = 1.29 + 0.506*log(DA)	35.8	73.59	33.28
log(25-yr Q) = 1.46 + 0.651*log (DA) − 0.411*log(BH)	26.71	88.19	23
log(50-year Q) = 1.39 + 0.597*log(DA)	32.19	82.89	29.42
log(100-year Q) = 1.41 + 0.631*log(DA)	35.59	81.6	32.55

Abbreviations: DA, drainage area in km^2; Q, peak flow in m^3/s; BH, basin shape factor (dimensionless).

from 9.6% to 12.2% across all basin sizes within our study. Figures 8b shows the result for the 25-year return period, for which basin area and shape factor were both significant variables. As shown in this figure, basin shape factor has the greatest influence in the percent change in peak flows. This is due to a greater difference in the basin shape factor model variables between Tables 2 and 3. As a whole, the change in peak flow predicted by applying regional flood frequency analysis to the Log Pearson III analysis in this study is important to consider as it produces the types of equations that are used within engineering designs to size bridges, culverts, and pipes and other types of flood conveyance infrastructure.

4 | DISCUSSION

We present a method to transfer flood risk from hurricanes to other regions within their probabilistic landfall path through the development of flood frequency statistics and regional regression equations. This method is applied in a case study to evaluate the impact that Hurricane Harvey would have had on flood frequency statistics and regional flood frequency analysis had its precipitation occurred in two different locations along the Texas gulf coast. Results indicated that Harvey would have increased the magnitude and frequency of most return periods floods, with the median 100-year flood increasing between 17% and 66%. These outcomes suggest that contemporary hurricanes may have an outsized influence on the estimation of the magnitude and frequency of peak flows and present several challenges for considering flood risk within engineering designs.

This study demonstrates that engineers and policymakers may need to account flood risk from climate enlarged hurricanes in all areas within their probabilistic landfall paths—not just where they occur. For example, the 25-year storm in a watershed in the central region with an area of 400 km^2 and a basin shape factor of 7 would increase from 538 m^3/s to 640 m^3/s if Harvey had it made landfall there. This increase of 102 m^3/s could translate into significant changes in infrastructure design, such as the flood height of a bridge or levee. This suggests that current infrastructure designs may be undersized, which supports the notion that traditional flood frequency methods fail to account for nonstationarity in precipitation extremes (Faulkner et al., 2020; Wright et al., 2019). While the results from our nonstationarity analysis demonstrate that streamflow

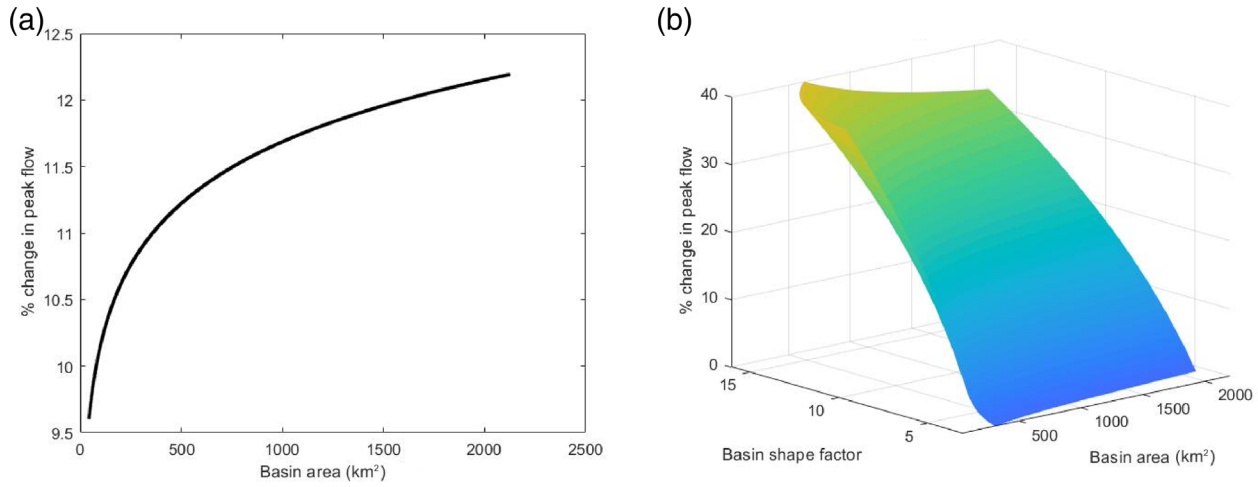

FIGURE 8 Central region percent change in RFF regression based upon the basin area for the 5-year return period (a) and based upon the basin area and basin shape factor for the 25-year return period (b)

records preceding Harvey had not been affected by changes in climate or land use at a statistically significant level, the impact of Harvey contradicts assumptions of stationarity. To that end, Hurricane Harvey is not a one-off event, as climate change is expected to increase the intensity of tropical cyclones and hurricanes (Knutson et al., 2010; Marsooli et al., 2019). Therefore, it would be prudent if future infrastructure is built in light of these larger storms, even in locations where the hurricane did not but could have made landfall.

While the method presented in this study clearly demonstrates how to transfer flood risk from a hurricane, doing so as a broad method to incorporate non-stationarity into flood frequency analysis has several limitations. These include the necessity of a recent extreme hurricane within the region, as well as uncertainties surrounding transposing precipitation data and translating that data to peak streamflow data through a model. As demonstrated through the Monte-Carlo simulation, there was an average coefficient of variation in the 3-day precipitation amount of 0.19 and 0.25 in the southern and central regions, respectively. This provides a general understanding of the uncertainty in rainfall distributions from transposing Harvey to these regions; however, there would certainly be other sources of uncertainty had Harvey made landfall in these regions due to differences the topography of the area, shape of the coastline, and land use, among other factors. Other methods could include a more comprehensive approach that tracks not only a single event, but a multitude of Gulf storms and their associated probable precipitation paths. In any case, an application of this method to quantify changes in flood frequency would need to acknowledge this uncertainty and how it may impact the interpretation of the results.

This method does not account for potential decreases in the frequency of tropical cyclones (Kirtman et al., 2013; Knutson et al., 2010) or increases in the frequency of other large rain events (Kirtman et al., 2013). The strength of this approach for engineering design is that it modifies an empirical method with observed storm events, rather than other methods to incorporate climate change into statistics for engineering design that rely on climate models or indices (Griffis & Stedinger, 2007; Srivastav et al., 2014). Furthermore, it has simple steps that can be taken apart and used with other methods where needed. For example, the previously mentioned Bayesian/Monte Carlo Markov Chain method (Ouarda & El-Adlouni, 2011) could be used to create inputs for the synthetic unit hydrographs used in this study.

The outcomes of this study support the need for research to incorporate nonstationarity into flood frequency analysis methods. To this end, engineers, scientists, and policymakers may find it helpful to utilize several methods to account for nonstationarity in flood frequency statistics. This will allow them to assemble a range of potential outcomes in a manner similar to how hurricane forecasters employ dozens of models when tracking a hurricane. Once a range of possible outcomes has been established, decision makers can choose a planning strategy that best fits their goals and risk tolerance. The City of Denver exemplified this approach when climate models predicted that precipitation contributing to their water supply may increase or decrease due to climate change (Waage & Kaatz, 2011). Therefore, this could be useful as one method among many for considering the influence of nonstationarity on flood frequency statistics.

5 | CONCLUSIONS

This study presents a method to transfer flood risk from hurricanes to other regions within their probabilistic landfall path through the development of flood frequency statistics and regional regression equations. To do so, we explored the impact that Hurricane Harvey could have had on flood frequency analysis and regional regression equations had its precipitation occurred elsewhere along the Texas coast. On average, our results show that simulating Harvey increased the 100-year peak flow by 17% and 66% in the central and southern geomorphologic regions along the Texas coast. Consequently, applying these return period peak flows in a regional regression study showed an average increase of 30.2% in the 100-year peak flow upon the incorporation of Hurricane Harvey simulations. These findings demonstrate that hurricanes that are intensified by climate change may significantly alter flood frequency statistics and regional regression equations in other regions within their probabilistic landfall paths. These changes in design floods have significant implications for the design of civil infrastructure for flood risk management.

ACKNOWLEDGMENTS

The authors would like to acknowledge the assistance of Adam Gottlieb for his work in organizing peak flow datasets for this study, as well as the assistance of Levi Cowan, Ph.D. candidate at Florida State University and author of tropicaltidbits.com, for help in developing our hurricane landfall probability maps.

DATA AVAILABILITY STATEMENT

Data has been uploaded to HydroShare, an online data repository operated by the Consortium of Universities for the Advancement of Hydrologic Science, Inc. (CUAHSI). The data can be accessed using the following information: Regier, E., W. McDonald, J. Naughton (2021). Data for "Method to Transfer Flood Risk and its Application to Hurricane Harvey", HydroShare, http://www.hydroshare.org/resource/db405313bb6e48a48cc601ee9893da46.

ORCID

Joseph Naughton https://orcid.org/0000-0002-5253-1992

Walter McDonald https://orcid.org/0000-0002-9217-7908

REFERENCES

Adib, A., Salarijazi, M., & Najafpour, K. (2010). Evaluation of synthetic outlet runoff assessment models. *Journal of Applied Sciences and Environmental Management*, *14*(3). https://doi.org/10.4314/jasem.v14i3.61450

Asquith, W. H., & Slade, R. M. J. (1997). *Regional equations for estimation of peak-Streamflow frequency for natural basins in Texas*. United States Geologic Survey. Retrieved from https://pubs.usgs.gov/wri/wri964307/pdf/wri4307.pdf

Automated Tropical Cyclone Forecasting System (ATCF). (2017). Index of /atcf/archive/2017. Retrieved from https://ftp.nhc.noaa.gov/atcf/archive/2017/.

Barth, N. A., Villarini, G., Nayak, M. A., & White, K. (2017). Mixed populations and annual flood frequency estimates in the western United States: The role of atmospheric rivers. *Water Resources Research*, *53*(1), 257–269.

Blake, E. S., & Zelinsky, D. A. (2017). Hurricane Harvey. Retrieved from https://www.nhc.noaa.gov/data/tcr/AL092017_Harvey.pdf.

Cook, J. L. (1987). Quantifying peak discharges for historical floods. *Journal of Hydrology*, *96*(1-4), 29–40.

Dawod, G. M., & Koshak, N. A. (2011). Developing GIS-based unit hydrographs for flood Management in Makkah Metropolitan Area, Saudi Arabia. *Journal of Geographic Information System*, *3*, 153–159. https://doi.org/10.4236/jgis.2011.32012

Dhakal, N., & Jain, S. (2019). Nonstationary influence of the North Atlantic tropical cyclones on the spatio-temporal variability of the eastern United States precipitation extremes. *International Journal of Climatology.*, *40*, 3486–3499. https://doi.org/10.1002/joc.6409

Di Baldassarre, G., & Montanari, A. (2009). Uncertainty in river discharge observations: A quantitative analysis. *Hydrology and Earth System Sciences*, *13*, 913–921 Retrieved from www.hydrol-earth-syst-sci.net/13/913/2009/

Eng, K., Chen, Y., & Kiang, J. E. (2010). Users guide to the weighted-multiple-linear regression program (WREG version 1.0). *United States geologic survey techniques and methods 4-A8*, U.S. Dept, of the Interior, U.S. Geological Survey. https://doi.org/10.3133/tm4A8

England, J. F., Cohn, T. A., Faber, B. A., Stedinger, J. R., Thomas, W. O. J., Veilleux, A. G., ... Mason, R. R. J. (2019). Guidelines for determining flood flow frequency bulletin 17C (ver 1.1, May 2019). In *U.S. Geological Survey techniques and methods, book 4*. United States Geological Survey https://doi.org/10.3133.

Esri Inc. (2017). *ArcMap*. Esri Inc. Retrieved from www.esri.com

Faulkner, D., Warren, S., Spencer, P., & Sharkey, P. (2020). Can we still predict the future from the past? Implementing non-stationary flood frequency analysis in the UK. *Journal of Flood Risk Management*, *13*(1), e12582.

Gao, S., & Fang, Z. (2018). Using storm transposition to investigate the relationships between hydrologic responses and spatial moments of catchment rainfall. *Natural Hazards Review*, *19*(4), 04018015.

Griffis, V. W., & Stedinger, J. R. (2007). Incorporating climate change and variability into bulletin 17B LP3 model. Retrieved from http://www.cpc.ncep.noaa.gov/data/indices/.

Günal, A. Y., & Güven, A. (2016). Synthetic unit hydrograph of small catchments by using GIS. *Acta Physica Polonica A*, *130*(1), 130–132. https://doi.org/10.12693/APhysPolA.130.130

Harmel, R. D., Cooper, R. J., Slade, R. M., Haney, R. L., & Arnold, J. G. (2006). Cumulative uncertainty in measured streamflow and water quality data for small watersheds. *Transactions of the ASABE*, *49*(3), 689–701. https://doi.org/10.13031/2013.20488

Hassanzadeh, P., Lee, C.-Y., Nabizadeh, E., Camargo, S. J., Ma, D., & Yeung, L. Y. (2020). Effects of climate change on the movement of future landfalling Texas tropical cyclones. *Nature Communications*, *11*(1), 1–9.

Helsel, D. R., & Hirsch, R. M. (2002). *Techniques of water-resources investigations of the United States geological survey book 4, hydrologic analysis and interpretation statistical methods in water resources* (Vol. 323). United States Geologic Survey. Retrieved from http://water.usgs.gov/pubs/twri/twri4a3/

Huttner, P. (2017). *Harvey poses potentially epic flood threat*. Minnesota Public Radio Retrieved from https://www.mprnews.org/story/2017/08/23/harvey-poses-potentially-epic-flood-threat

Jarrett, R. D. (1987). Errors in slope-area computations of peak discharges in mountain streams. *Journal of Hydrology*, *96*(1-4), 53–67.

Kirtman, B., Power, S. B., Adedoyin, J. A., Boer, G. J., Bojariu, R., Camilloni, I., ... Wang, H. J. (2013). Near-term climate change: Projections and predictability. In P. Deleclus, T. Palmer, T. Shepherd, & F. Zwiers (Eds.), *Climate change 2013: The physical science basis. Contribution of working group I to the fifth assessment report of the intergovernmental panel on climate change* (pp. 953–1028). Cambridge University Press.

Knutson, T. R., McBride, J. L., Chan, J., Emanuel, K., Holland, G., Landsea, C., ... Sugi, M. (2010). Tropical cyclones and climate change. *Nature Geoscience*, *3*(3), 157–163.

Kuczera, G. (1996). Correlated rating curve error in flood frequency inference. *Water Resources Research*, *32*(7), 2119–2127.

Marsooli, R., Lin, N., Emanuel, K., & Feng, K. (2019). Climate change exacerbates hurricane flood hazards along US Atlantic and Gulf Coasts in spatially varying patterns. *Nature Communications*, *10*(1), 1–9. https://doi.org/10.1038/s41467-019-11755-z

McCuen, R. H., & Galloway, K. E. (2010). Record length requirements for annual maximum flood series. *Journal of Hydrologic Engineering*, *15*(9), 704–707.

McDonald, W. M., & Naughton, J. B. (2018). Impact of hurricane Harvey on the results of regional flood frequency analysis. *Journal of Flood Risk Management*, *e12500*. https://doi.org/10.1111/jfr3.12500

Ouarda, T. B. M. J., & El-Adlouni, S. (2011). Bayesian nonstationary frequency analysis of hydrological Variables1. *JAWRA Journal of the American Water Resources Association*, *47*(3), 496–505. https://doi.org/10.1111/j.1752-1688.2011.00544.x

Pettitt, A. N. (1979). A non-parametric approach to the change-point problem. *Journal of the Royal Statistical Society. Series C (Applied Statistics)*, *28*(2), 126–135 Retrieved from https://0-www-jstor-org.libus.csd.mu.edu/stable/pdf/2346729.pdf?ab_segments=0%252Fdefault-2%252Fcontrol&refreqid=excelsior%3A71c89fea2b22a3c3d987f22546ef0ceb.

Ponce, V. M. (1989). *Engineering hydrology: Principles and practices* (Vol. 640). Pearson College Div.

Rallison, R. E., Newton, D. W., Miller, J. F., Delk, R. G., Rawls, W. J., & Hagen, V. K. (1981). *Guidelines for determining flood flow frequency: Bulletin #17B of the hydrology subcommittee*. United States Geologic Survey. Retrieved from https://water.usgs.gov/osw/bulletin17b/dl_flow.pdf

Reed, K. A., Stansfield, A. M., Wehner, M. F., & Zarzycki, C. M. (2020). Forecasted attribution of the human influence on Hurricane Florence. *Science Advances*, *6*(1), 1–9.

Reshma, T., Sundara Kumar, P., Ratna, M. J., Babu, K., & Sundara Kumar, K. (2010). Simulation of runoff in watersheds using SCS-CN and Muskingum-Cunge methods using remote sensing and geographical information systems. *International Journal of Advanced Science and Technology*, *25*, 31–42 Retrieved from https://pdfs.semanticscholar.org/8437/a37b387f3d7b5575572c5a7b95fff9281585.pdf

Risser, M. D., & Wehner, M. F. (2017). Attributable human-induced changes in the likelihood and magnitude of the observed extreme precipitation during Hurricane Harvey. *Geophysical Research Letters*, *44*(24), 12–457.

Sheets, R. C. (1985). The national weather service hurricane probability program. *Bulletin of the American Meteorological Society*, *66*(1), 4–13. https://doi.org/10.1175/1520-0477(1985)066<0004:TNWSHP>2.0.CO;2

Srivastav, R. K., Schardong, A., & Simonovic, S. P. (2014). Equidistance quantile matching method for updating IDFCurves under climate change. *Water Resources Management*, *28*(9), 2539–2562. https://doi.org/10.1007/s11269-014-0626-y

Sule, B. F., & Alabi, S. A. (2013). Application of synthetic unit hydrograph methods to construct storm hydrographs. *International Journal of Water Resources and Environmental Engineering*, *5*(11), 639–647. https://doi.org/10.5897/IJWREE2013.0437

Turnipseed, P., & Sauer, V. B. (2010). *Discharge measurements at gaging stations chapter 8 of book 3, Section A*. United States Geologic Survey. Retrieved from https://pubs.usgs.gov/tm/tm3-a8/pdf/tm3-a8.pdf

U. S. Geological Survey (2019a). The National Map—New data delivery homepage, advanced viewer, lidar visualization. Retrieved from https://pubs.er.usgs.gov/publication/fs20193032.

U. S. Geological Survey (2019b). USGS Current Conditions for Texas. Retrieved from https://waterdata.usgs.gov/tx/nwis/uv?.

van Oldenborgh, G. J., van der Wiel, K., Sebastian, A., Singh, R., Arrighi, J., Otto, F., ... Cullen, H. (2017). Attribution of extreme rainfall from Hurricane Harvey, August 2017. *Environmental Research Letters*, *12*(12), 124009. https://doi.org/10.1088/1748-9326/aa9ef2

Veilleux, A. G., Cohn, T. A., Flynn, K. M., Mason, R. R., & Hummel, P. R. (2013). Estimating magnitude and frequency of floods using the PeakFQ 7.0 program. 10.3133/fs20133108

Villarini, G., Serinaldi, F., Smith, J. A., & Krajewski, W. F. (2009). On the stationarity of annual flood peaks in the continental United States during the 20th century. *Water Resources Research*, *45*(8).

Villarini, G., Smith, J. A., Baeck, M. L., & Krajewski, W. F. (2011). Examining flood frequency distributions in the Midwest US 1. *JAWRA Journal of the American Water Resources Association*, *47*(3), 447–463.

Vogel, R. M., Yaindl, C., & Walter, M. (2011). Nonstationarity: Flood magnification and recurrence reduction factors in the United States. *JAWRA Journal of the American Water Resources Association*, *47*(3), 464–474. https://doi.org/10.1111/j.1752-1688.2011.00541.x

Vu, T. M., & Mishra, A. K. (2019). Nonstationary frequency analysis of the recent extreme precipitation events in the United States. *Journal of Hydrology*, *575*, 999–1010.

Waage, M. D., & Kaatz, L. (2011). Nonstationary water planning: An overview of several promising planning methods. *JAWRA Journal of the American Water Resources Association*, *47*(3), 535–540. https://doi.org/10.1111/j.1752-1688.2011.00547.x

Wright, D. B., Bosma, C. D., & Lopez-Cantu, T. (2019). US hydrologic design standards insufficient due to large increases in frequency of rainfall extremes. *Geophysical Research Letters*, *46*(14), 8144–8153.

Wright, D. B., Smith, J. A., & Baeck, M. L. (2014). Flood frequency analysis using radar rainfall fields and stochastic storm transposition. *Water Resources Research*, *50*(2), 1592–1615.

Wright, D. B., Smith, J. A., Villarini, G., & Baeck, M. L. (2013). Estimating the frequency of extreme rainfall using weather radar and stochastic storm transposition. *Journal of Hydrology*, *488*, 150–165.

How to cite this article: Regier, E., Naughton, J., & McDonald, W. (2021). Transposing flood risk from extreme rainfall events: A case study of Hurricane Harvey. *Journal of Flood Risk Management*, e12778. https://doi.org/10.1111/jfr3.12778